ELSEVIER

Magnetic Resonance Imaging 18 (2000) 485–488

MAGNETIC RESONANCE IMAGING

Technical Note

Automatic localization of EEG electrode markers within 3D MR data

J. Sijbers[a,*], B. Vanrumste[b], G. Van Hoey[b], P. Boon[c], M. Verhoye[d], A. Van der Linden[d], D. Van Dyck[a]

[a]*Vision Lab, University of Antwerp, Antwerp, Belgium*
[b]*MEDISIP, University of Ghent, Ghent, Belgium*
[c]*Neurology Department, University of Ghent, Ghent, Belgium*
[d]*Bio-Imaging Lab, University of Antwerp, Antwerp, Belgium*

Abstract

The electrical activity of the brain can be monitored using ElectroEncephaloGraphy (EEG). From the positions of the EEG electrodes, it is possible to localize focal brain activity. Thereby, the accuracy of the localization strongly depends on the accuracy with which the positions of the electrodes can be determined. In this work, we present an automatic, simple, and accurate scheme that detects EEG electrode markers from 3D MR data of the human head.

Keywords: Automatic; EEG electrodes; Markers; Localization; Detection; MR; 3D

1. Introduction

Over the past few years, interest in combining EEG and magnetic resonance imaging (MRI) has grown considerably. Technical advances in the development of EEG recording systems suited for MRI nowadays even allows simultaneous MRI/EEG acquisition [1–5]. Due to their complementary strengths, the combination of the two techniques is able to render a new and powerful tool in functional brain research. With functional MRI (fMRI), the localization of activated areas can be determined with very high accuracy. The time resolution of fMRI, however, is rather poor and thereby it is not adequate to fully explore the complex dynamics of neural processes. In contrast to fMRI, the time resolution of EEG is excellent but the resolution of spatial source allocation is low. Therefore, combining these two modalities is helpful in the study of the brain. Indeed,

1. Using the anatomical information from a 3D high resolution MR image allows to build a realistically shaped conductivity model of the head to obtain a more accurate spatial localization of the EEG sources.
2. Combining both the information from functional MRI and from the EEG findings can give more insight into the functioning of the brain.

The first item is constituted of many steps, one of which is detection of the EEG electrodes in the MR image. In this note, we present a practical method for automatic, spatial localization of EEG electrodes in a 3D high-resolution MR image.

Previous reported techniques for localization of marked EEG electrodes employed manual as well as (semi-)automatic segmentation [6–9]. Van Hoey et al.[8] presented a scheme based on correlation with a disc-shaped template to detect spherically shaped markers. Thereby, false positives are reduced using shape criteria for the marker candidates. However, still a significant amount of erroneous detected markers remain, such that posterior user interaction is needed. Wang et al. described an automatic scheme for the detection of markers in computed tomograph and MR images, which are used for geometrical image registration [6]. A similar technique was employed by Brinkmann et al. for registration of a 3D MR image to data from a magnetic digitizer [9]. In both papers, morphological operations are used to segment the markers from 3D MR data of the human head. One step of the segmentation consists of an opening operation to remove the markers. The resulting mask is then excluded from the marker search space. However, to our experience, the mask created this way is rather poor due to the presence of dark intensity areas within the head, which can only partly be solved by posterior closing operations. In

* Corresponding author. Groenenborgerlaan 171, B-2020 Antwerp, Belgium. Tel.: +32-(0)3-218-0-452; fax: +32-(0)3-218-0-318.
E-mail address: sijbers@ua.ac.be (J. Sijbers).

0730-725X/00/$ – see front matter
PII: S0730-725X(00)00121-1

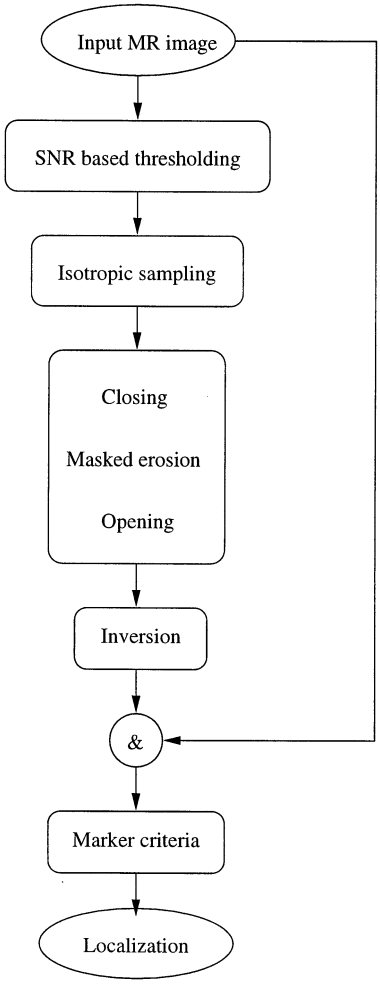

Fig. 1. Flowchart of the EEG electrode localization scheme.

this paper, we show how this step can significantly be improved, by means of a simple modification to the morphological operations. All steps are applied in 3D and are fully automatic.

2. Methods

In this section, the procedure for the electrode localization is outlined. For a schematic view, we refer to Fig. 1.

2.1. Foreground separation

The first step of the marker detection procedure is thresholding of the 3D MR data set as to separate the foreground from the background. The greylevel threshold value must be chosen as low as possible to ensure selection of all markers. On the other hand, the threshold value should be set as high as possible as to put as many background noise pixels as possible to zero. Clearly, this is an optimality problem, based on the image noise variance which needs to be estimated from the available MR data.

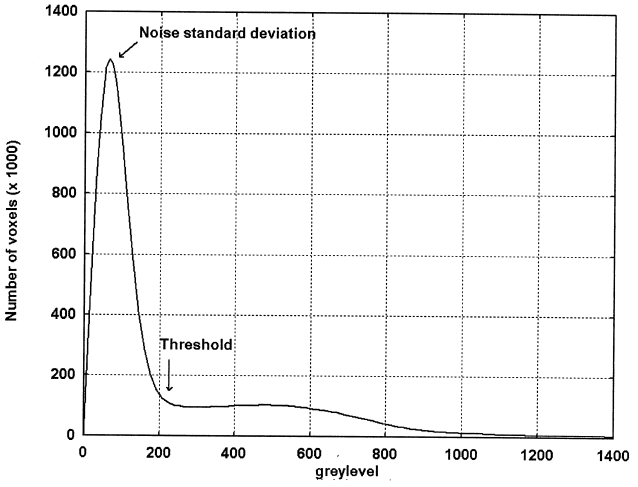

Fig. 2. Typical histogram of a 3D MR data set of a human head.

In the past, many techniques have been proposed for noise estimation of MR data which are based on finding homogeneous regions [10,11] or an a double acquisition scheme [12]. In the proposed scheme, the noise is automatically estimated from the histogram of the 3D MR data set (see Fig. 2). The histogram is constituted of the Rayleigh distributed image background pixels and the Rice distributed foreground pixels. Thereby, the background's Rayleigh distribution is almost always clearly differentiated from the foreground modes such that the noise standard deviation can directly be derived from the maximum of the Rayleigh distribution. Apart from ease of automatization, this technique has the advantage to be insensitive to inhomogeneities in the background area.

Based on the estimated noise standard deviation $\hat{\sigma}$, the input data is thresholded at $3.5\hat{\sigma}$, thereby setting 99.8% of the background pixel values to zero. Fig. 3a shows a sagittal slice of the 3D data set, in which two markers are clearly visible. The result of the thresholding is shown in Fig. 3b.

2.2. Morphological operations

Having thresholded the input image and thereby producing a binary image, the next step is to exclude the head area from the non-zero voxels while retaining the marker areas. This is done by means of morphological image operations, which were constructed to act isotropically in three dimensions. Therefore, prior to the morphology, the image data set is resampled to obtain a spatially isotropic data set. The applied morphological operations consist of a masked erosion after a closing operation, followed by an opening.

Closing

The thresholding does not turn the whole head area into foreground voxels due to the presence of low intensity areas such as the skull or sinuses. In order to fill the interior of the head, a 3D closing operation was performed with a 26-con-

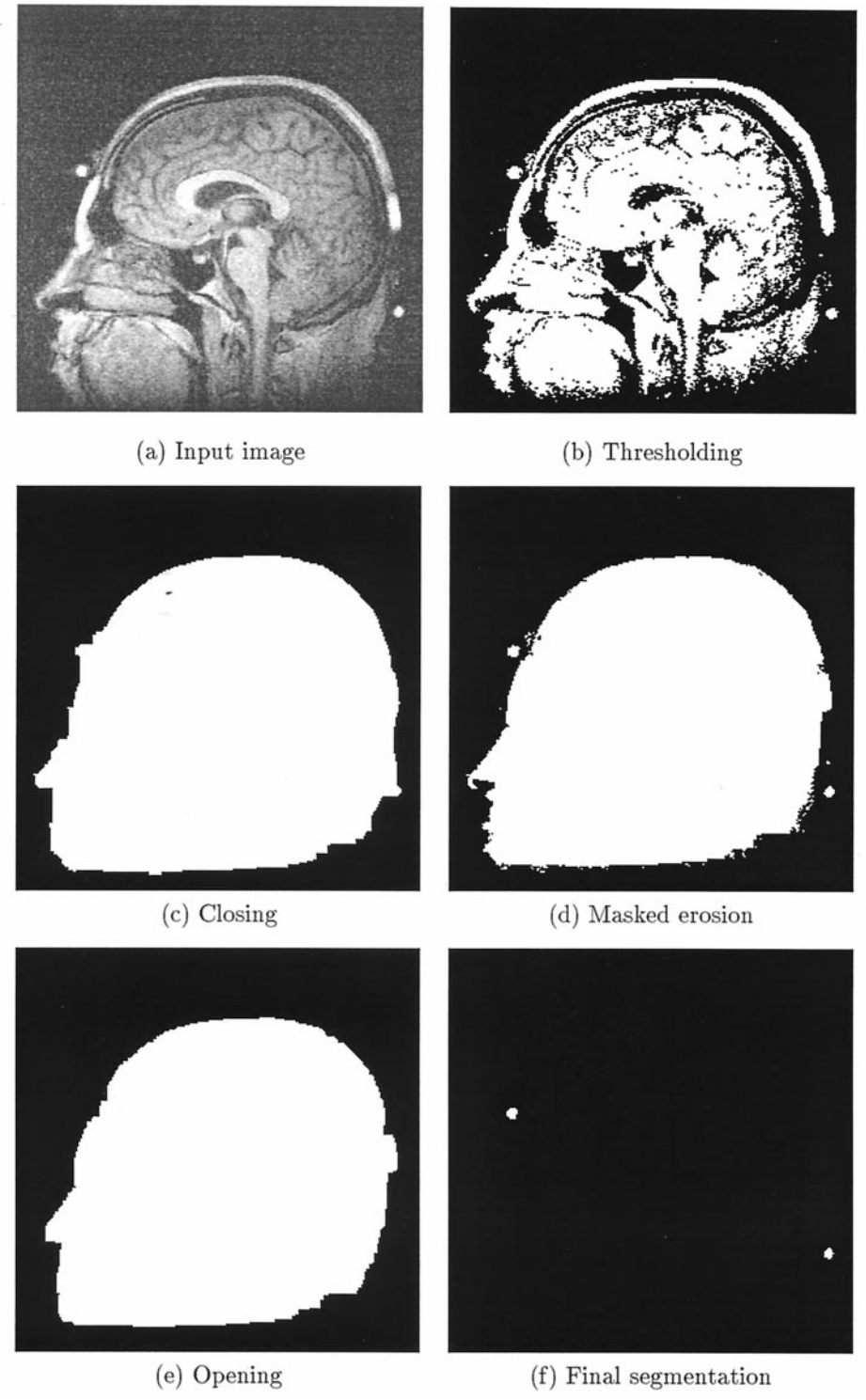

Fig. 3. Sagittal image demonstrating the output of the marker detection steps: thresholding (b), closing (c), masked erosion (d), opening (e) and the result of marker shape criteria (f).

nected neighborhood (i.e., a number of dilations, followed by an identical number of erosions). The result is shown in Fig. 3c. The figure clearly shows that the void head areas are filled, but also that the markers are merged with the head area.

Masked erosion

To recover the marker disconnection without affecting the closing result within the head area, a number of 3D erosion operations was applied during which the original

binary image (Fig. 3b) was kept fixed. The result of this stage can be appreciated from Fig. 3d.

Opening

Owing to the previous step, segmentation of the markers becomes obvious. Indeed, application of a 3D opening operation now results in the removal of the markers (see Fig. 3e). This is the head mask that should be excluded from the marker search space.

2.3. Marker localization

The morphological operations lead to a mask that, after inversion, is logically multiplied with the input image. All remaining objects are then labeled and subjected to selection criteria such volume, average intensity, spatial distribution, etc. This step removes spurious noise pixels and non-spherical objects such as parts of the ear or MRI artifacts. Final spatial coordinates $\{x_j^c\}$ of the markers are obtained by computing the intensity weighted centroids [6]:

$$x_j^c = \frac{\sum_i \sqrt{I_i^2 - 2\hat{\sigma}^2}\, x_{i,j}}{\sum_i \sqrt{I_i^2 - 2\hat{\sigma}^2}} \quad j = 1, 2, 3 \tag{1}$$

where I_i denotes the magnitude intensity of voxel i within the marker. Note that I_i^2 is subtracted by $2\hat{\sigma}^2$ to reduce the bias introduced by the Rice statistics of the magnitude data [13].

3. Results and discussion

3D MR images were acquired of a human head on which various electrodes were attached, marked with 27 spherically shaped Vitamin A markers (Lambo, 8 mm).

The morphological part of the marker detection scheme leads to a mask containing the full head area within the skin, hence leading to a reduced risk of wrongly localized EEG electrodes. The fact that during the erosion stage the original thresholded image was kept fixed, is an important difference compared to a conventional closing operation. Such a closing operation would not be able to isolate the electrode markers but would lead to merging of the markers with the head area.

Concerning computational requirements, the morphological operations were efficiently implemented using border queues. Thereby, only voxels lying on the border were processed and neighboring voxels affected by the operation were added to the queue. The whole procedure took about 80 s on a Pentium 400 MHz. Application of the above marker detection scheme revealed detection of all markers fully lying within the data set. Markers partially contained within the data set were not always detected. The percentage of false positives was about 2%.

4. Conclusions

In this work, a simple and automatic scheme was presented for the detection of spherically shaped markers within a 3D MRI data set. A small number of false positives could be obtained by reduction of the marker search space using morphological image operations.

Acknowledgements

This work was financially supported by the Flemish institute for the promotion of scientific and technological research in the industry (IWT), Brussels, and by the EC CRAFT project Nr. BES2-5214.

References

[1] Gevins A, Brickett P, Costales B, Le J, Reutter B. Beyond topographic mapping: towards functional-anatomical imaging with 124-channel EEGs and 3D MRIs. Brain Topography 1990;3:53–64.
[2] Ives JR, Warach S, Schmitt F, Edelman RR, Schomer DL. Monitoring the patients' EEG during echo planar MRI. Clin Neurol 1993;87:417–20.
[3] Warach S, Ives JR, Schlaug G, Patel MR, Darby DG, Thangaraj V, Edelman RR, and Schomer DL. EEG-triggered echo-planar functional MRI in epilepsy. Neurology 1996;47:89–93.
[4] Busch E, Hoehn-Berlage M, Eis M, Gyngell ML, Hossman KA. Simultaneous recording of EEG, DC potential and diffusion-weighted NMR imaging during potassium induced cortical spreading depression in rats. NMR Biomed 1995;8:59–64.
[5] Huang-Hellinger FR, Heiter HC, McGormack G, Cohen MS, Kwong KK, Sutton JP, Savoy RL, Weiskoff RM, Davis TL, Baker JR, Belliveau JW, Rosen BR. Simultaneous functional magnetic resonance imaging and electrophysiological recording. Human Brain Mapping 1995;3:13–23.
[6] Wang MY, Maurer CR, Fitzpatrick JM, Maciunas RJ. An automatic technique for finding and localizing externally attached markers in CT and MR volume images of the head. IEEE Trans Biomed Engineer 1996;43:627–37.
[7] Yoo SS, Guttmann CRG, Ives JR, Panych LP, Kikinis R, Schomer DL, Jolesz FA. 3D localization of surface 10–20 EEG electrodes on high resolution anatomical MR images. Electroencephalograph Clin Neurophysiol 1997;102:335–339.
[8] Van Hoey G, Vanrumste B, Van de Walle R, Boon P, Lemahieu I. Automatic marker recognition on MR images for EEG electrode localization. In Proceedings of the ProRISC/IEEE Benelux Workshop on Circuits, Systems and Signal Processing, CSSP 97, Mierlo, 1997. p. 625–30.
[9] Brinkmann BH, O'Brien TJ, Dresner MA, Lagerlund TD, Sharbrough FW, Robb RA. Scalp-recorded EEG localization in MRI volume data. Brain Topography 1998;10:245–53.
[10] Henkelman RM. Measurement of signal intensities in the presence of noise in MR images. Med Phys 1985;12:232–3.
[11] Sijbers J, den Dekker AJ, Verhoye M, Van Audekerke J, Van Dyck D. Estimation of noise from magnitude MR images. Magnetic Resonance Imaging 1998;16:87–90.
[12] Sijbers J. Estimation of Signal and Noise from Magnitude MR Images. PhD thesis, University of Antwerp, May 1998. Info: http://wcc.ruca.ua.ac.be/~visielab/sijbers/thesis.html.
[13] Sijbers J, den Dekker AJ, Scheunders P, Van Dyck D. Maximum likelihood estimation of Rician distribution parameters. IEEE Trans Med Imaging 1998;17:357–61.